ADVANCED FUNCTIONAL MATERIALS
www.afm-journal.de

Surface Modification of Silicone with Covalently Immobilized and Crosslinked Agarose for Potential Application in the Inhibition of Infection and Omental Wrapping

Min Li, Koon-Gee Neoh, En-Tang Kang, Titus Lau,and Edmund Chiong*

In peritoneal dialysis (PD), the catheter, usually made of silicone, has been considered the "lifeline" of the patient. However, the PD catheter also serves as a nidus for bacterial infection. Furthermore, complications can result from fibrin deposition and omental wrapping of the catheter, which obstructs the dialysate flow. In this work, a crosslinked agarose (AG) polymer layer is covalently grafted as a microscale coating on the silicone surface. This coating reduces *Staphylococcus aureus, Escherichia coli*, and *Pseudomonas aeruginosa* biofilm formation by more than two orders of magnitude. In addition, cell and platelet adhesion and protein adsorption is also reduced by ≥90%. Without compromising the antibacterial and antifouling property, further improvement in hemocompatibility, as shown by the inhibition of platelet adhesion and activation, prolonged plasma recalcification time and lower hemolysis degree, is achieved by co-immobilization of 2.6 μg cm^{-2} of heparin (HEP) in the agarose coating. The AG–HEP coatings are not cytotoxic to mammalian cells, and are stable for extended periods in lysozyme aqueous solution and under autoclaving at 121 °C for 20 min.

1. Introduction

Peritoneal dialysis (PD) is an effective home-based dialysis treatment modality for patients with severe renal disease, and it has been used in many countries as a significantly lower cost alternative to hemodialysis.[1,2] However, the success of PD may be compromised by complications related to the catheter, which is usually made of silicone. Biofouling (in the form of protein adsorption and cell adhesion) and bacterial attachment on the highly hydrophobic silicone surface may result in omental wrapping and infection, which is the leading cause of PD outflow failure and the second most common cause of death for PD patients, respectively.[3–6] In addition, when in contact with blood, platelet adhesion and activation-induced thrombosis may lead to intraluminal obstruction of PD catheters.[7] The PD catheter can be considered the "lifeline" of the PD patient, and catheter-related complications are the primary obstacle to the widespread use of PD. Since the introduction of Tenckhoff catheter in mid-1960s, the development of new PD catheter designs has not shown convincing improvement in reducing infection and increasing the survival rates of PD patients.[8] Thus, in recent years, modification of the catheter surface to improve its antifouling, antibacterial and hemocompatible properties has attracted increasing interest.[9–13]

Tethering of functional polymer coatings via covalent bonding provides an effective way to modify catheter surface properties.[14–17] The synthetic hydrophilic polymer, poly(ethylene glycol) (PEG), and its derivatives are the most widely used antifouling and antibacterial materials.[18,19] However, PEG suffers from some limitations: PEG-coated surfaces are unable to reduce protein adsorption to very low levels due to their interactions with proteins, and they are also susceptible to oxidative degradation in the presence of oxygen and transitional metal ions which limits its long-term antifouling and antibacterial performance in vivo.[20,21] Other synthetic polymers such as poly(acrylamide)s,[22,23] poly(sulfobetaine methacrylate),[24–26] poly(carboxybetaine methacrylate)[27] and poly(peptoid)s[28,29] are extensively investigated for use as antifouling coatings. Natural polymers, as compared with their synthetic counterparts derived from petrochemicals, provide an attractive alternative. Chitosan and its derivatives are the most widely used natural polymers for antibacterial coatings,[30–32] but their antifouling properties are limited because of their strong interactions with proteins.[33,34] Heparin (HEP), a commonly-used anticoagulant agent, has been reported to be an antibacterial coating which can reduce infection both in vitro and in vivo.[35] However, the antibacterial effect of HEP is still debatable. Some studies reported that HEP did not significantly reduce biofilm formation by *S. aureus* and may even stimulate the process.[36,37] Immobilization of protein-degrading enzymes, such

Dr. M. Li, Prof. K.-G. Neoh, Prof. E.-T. Kang
Department of Chemical
and Biomolecular Engineering
National University of Singapore
Kent Ridge, Singapore, 117576
E-mail: chenkg@nus.edu.sg
Dr. T. Lau, Dr. E. Chiong
National University Hospital
Kent Ridge, Singapore, 117576

DOI: 10.1002/adfm.201302242

as Subtilisin A, was found to reduce protein adsorption on surfaces.[38,39] At present, surface modification of silicone with covalently immobilized natural polymer coatings for the long-term improvement of its antifouling, antibacterial and hemocompatible properties is lacking.

Agarose (AG) is a neutral polysaccharide, which is derived from agar. As a US Food and Drug Administration (FDA)-approved ingredient, AG is widely used in many fields of biomedical applications, such as nerve regeneration, drug and gene delivery, and dental impression due to its biocompatibility, stability and inertness.[40–42] In earlier reports, AG, in the form of film and hydrogel, was shown to resist *Proteus mirabilis* bacterial adhesion[43] and marine fouling.[44] In this study, modification of AG by the introduction of acrylate groups was carried out to facilitate a covalently immobilized and crosslinked AG layer on medical grade silicone film and catheter surfaces to improve their antibacterial and antifouling properties. A problem frequently encountered in silicone surface modification is hydrophobic recovery, which is caused by the re-orientation and migration of the hydrophobic silicone segments and the coating polymer, due to the high flexibility and low glass transition temperature of the silicone polymer.[45] The agarose coating in this work was crosslinked to prevent hydrophobic recovery and improve its stability. In addition, HEP modified with methacrylate groups was covalently incorporated into the crosslinked AG layer to further improve the silicone's hemocompatibility. Protein adsorption, bacterial colonization, and cell and platelet adhesion on the AG and AG–HEP modified silicone were evaluated in vitro.

2. Results and Discussion

2.1. Surface Characterization

The procedures for the covalent grafting and crosslinking of AG and AG–HEP polymers on the silicone surfaces are illustrated schematically in **Figure 1**. The peroxides and hydroxyl peroxides on the silicone surface generated by oxygen plasma or ozone treatment served as anchor sites for the subsequent immobilization of the polymer chains.[46] The X-ray photoelectron spectroscopy (XPS) widescan, S 2p core-level and N 1s core-level spectra of the AG, HEP, and AG–HEP grafted silicone films are shown in **Figure 2**. The intensity of the Si 2p and Si 2s signals in the widescan spectrum of the crosslinked AG grafted silicone film, Silicone-*g*-AG4, (Figure 2(a)) is significantly decreased as compared to that of the pristine silicone film (Figure S1(a), Supporting Information), indicating the successful grafting of AG on the silicone film. As expected, no sulfur and nitrogen signals are discernible in the S 2p core-level and N 1s core-level spectra of the Silicone-*g*-AG4 film (Figure 2(a′) and its inset, respectively) since these elements are not present in silicone or acrylated AG polymer. The surface elemental compositions of the pristine and polymer-modified silicone as determined by XPS are shown in **Table 1**. The [Si]/[C] ratio of the Silicone-*g*-AG4 film is about 0.08:1 and is much lower than that of the pristine silicone (0.52:1). The extent of AG grafting can be qualitatively estimated from the [Si]/[C] ratio since Si is present only in silicone and not in the acrylated AG. As shown in Table 1, the [Si]/[C] ratios of Silicone-*g*-AG1, Silicone-*g*-AG2, Silicone-*g*-AG3 and

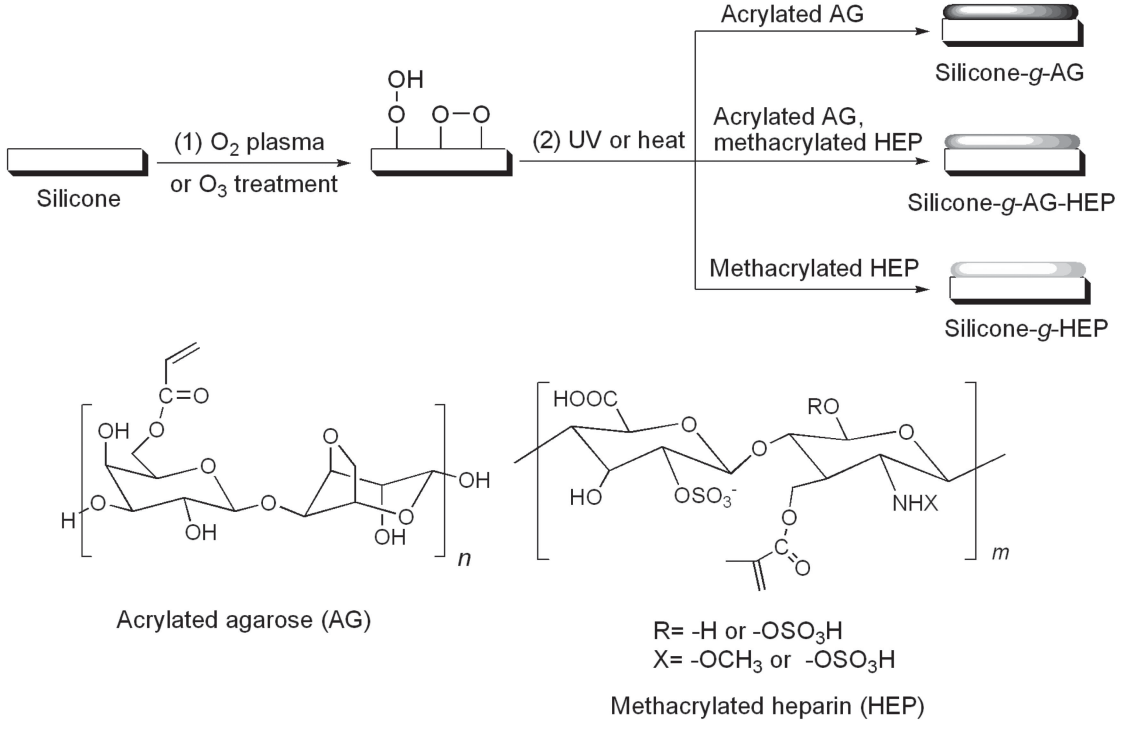

Figure 1. Schematic illustration of the modification of silicone surface via oxygen plasma or ozone treatment (Step (1)), and UV or heat-induced immobilization and crosslinking of acrylated AG and methacrylated HEP (Step (2)).

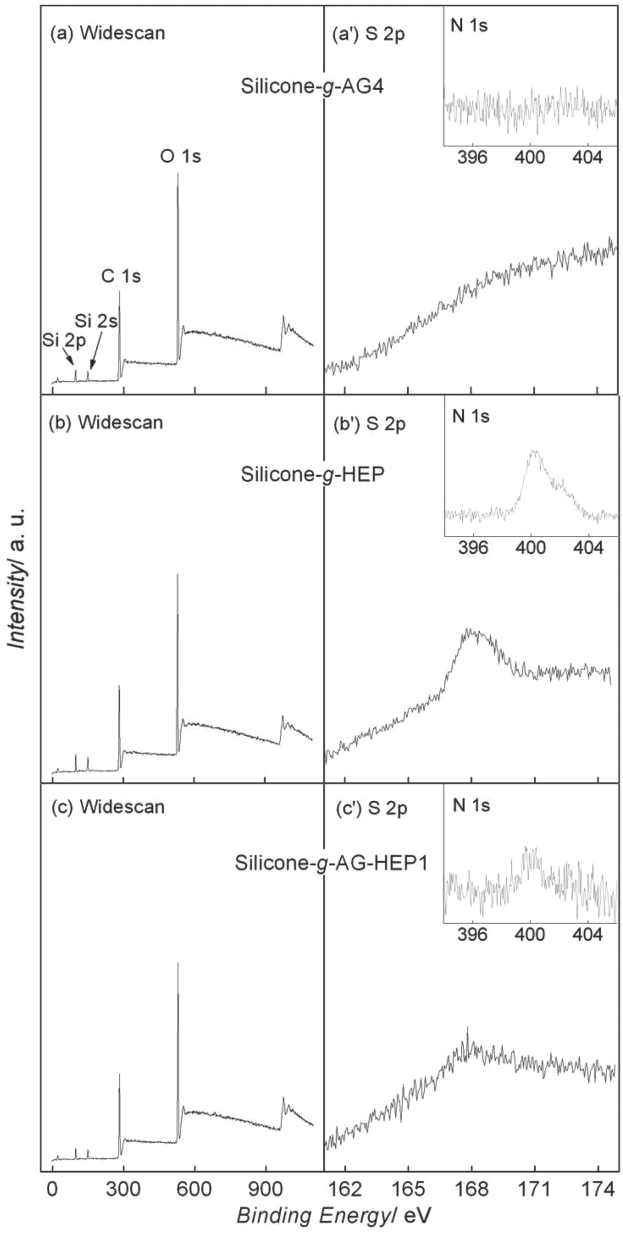

Figure 2. XPS widescan and S 2p core-level spectra of the a,a') Silicone-*g*-AG4, b,b') Silicone-*g*-HEP, and c,c') Silicone-*g*-AG-HEP1 films. The insets show the N 1s core-level spectrum of respective film.

Silicone-*g*-AG4 films decrease with increasing UV irradiation time from 15 min to 120 min, indicating an increase in the grafting density of the immobilized AG.

For the HEP modified silicone film, Silicone-*g*-HEP, sulfur and nitrogen signals are present in the S 2p core-level and N 1s core-level spectra (Figure 2(b') and its inset, respectively) after 120 min of UV-induced grafting of methacrylated HEP. In addition, the [Si]/[C] ratio of the Silicone-*g*-HEP film decreased to 0.14:1, which also confirms the successful grafting of HEP on the silicone film. The surface concentration of immobilized HEP, as determined by the toluidine blue method, was 12.1 μg cm^{-2} of the Silicone-*g*-HEP film.

For the silicone film modified with both AG and HEP, Silicone-*g*-AG-HEP1, the sulfur and nitrogen signals are discernible in the S 2p core-level and N 1s core-level spectra (Figure 2(c') and its inset, respectively). The [Si]/[C] ratio of the Silicone-*g*-AG-HEP1 film decreased to 0.10:1. **Figure 3** shows the field emission scanning electron microscopy (FESEM) images of the cross-section of the AG and AG-HEP modified films. It can be clearly observed that the thickness of the grafted AG layer (upper layer in Figure 3(a)) on Silicone-*g*-AG4 (120 min of UV irradiation), and the AG–HEP layer (upper layer in Figure 3(b)) on Silicone-*g*-AG-HEP1 (120 min of UV irradiation) is ~2 μm, confirming the successful grafting of AG and AG–HEP on the silicone surface. The thickness of the grafted AG layer can be varied by changing the the UV irradiation time. When the UV irradiation time was decreased to 60 min and 15 min, the thickness of the grafted AG layer decreased to 0.8 μm and 0.3 μm, respectively. The surface concentration of the immobilized HEP increased with increasing feed ratio of methacrylated HEP in the reaction solution (compare the immobilized HEP concentration of Silicone-*g*-AG-HEP1 and Silicone-*g*-AG-HEP2 in Table 1), which is also confirmed by the increase in [S]/[C] and [N]/[C] ratios of these films in Table 1.

The change in water contact angle of the pristine and polymer-modified silicone also provides supporting evidence that the silicone film surface has been successfully modified. As shown in Table 1, the pristine silicone film is hydrophobic with a water contact angle of 107°. The modified silicone films after grafting with AG, HEP, and AG–HEP became more hydrophilic with a much lower water contact angle. In addition, it can be observed that the contact angle of the AG-modified silicone films decreases with increasing UV reaction time, indicating an increase in the grafting density of the immobilized AG, which is consistent with the results revealed by the surface [Si]/[C] ratios of these films (Table 1).

2.2. Bacterial Adhesion and Biofilm Formation Assay

Development of surface resistance to bacterial adhesion is a crucial step to prevent bacterial infection. After adhesion on a surface, bacteria will multiply and form biofilm in the presence of a growth medium. The biofilm in turn protects the bacterial cells from the host's natural defense systems as well as antibiotics.[47] For an implanted device, such as a PD catheter, the first few hours after insertion is considered an important period where the introduced pathogen is still in the quiescent stage and the host immune system can actively neutralize the invading pathogen. The efficacy of the polymer-modified silicone film in reducing bacterial adhesion was evaluated using the model bacteria, Gram-positive *S. aureus* and Gram-negative *E. coli*, because they are among the most common species responsible for PD-related infections.[4] **Figure 4** shows the scanning electron microscopy (SEM) images of adherent *S. aureus* cells on pristine and modified silicone films. A large number of *S. aureus* was observed on pristine silicone after 4 h of incubation in phosphate buffer saline (PBS) (Figure 4(a)). The number of adherent *S. aureus* was significant reduced after surface modification of the silicone film with AG, AG–HEP, and HEP (Figure 4(b–d)). It is well-known that microbes prefer

Table 1. Surface composition and water contact angle of the polymer-modified silicone films.

Sample	Acrylated AG/ methacrylated HEP feed ratio [w/w%]	Reaction time [min]	[C]:[Si]:[S]:[N][a]	Water contact angle [±3°]	Heparin concentration [μg cm^{-2}][b]
Pristine silicone	–	–	1:0.52:-:-	107	–
Silicone-*g*-AG1[c]	100/0	15	1:0.31:-:-	42	–
Silicone-*g*-AG2[c]	100/0	30	1:0.22:-:-	35	–
Silicone-*g*-AG3[c]	100/0	60	1:0.15:-:-	34	–
Silicone-*g*-AG4[c]	100/0	120	1:0.08:-:-	30	–
Silicone-*g*-AG–HEP1[d]	90/10	120	1:0.10:0.0081:0.0036	29	2.6 ± 0.9
Silicone-*g*-AG–HEP2[d]	80/20	120	1:0.12:0.0090:0.0040	33	4.7 ± 0.6
Silicone-*g*-HEP[e]	0/100	120	1:0.14:0.015:0.0090	40	12.1 ± 1.9

[a][C]:[Si]:[S]:[N] molar ratio calculated from the sensitivity factor-corrected XPS C 1s, Si 2p, S 2p and N 1s core-level spectral area ratio; [b]Surface concentration of immobilized HEP on the AG–HEP modified silicone films as determined by the toluidine blue method; [c]AG-grafted silicone prepared by UV-induced immobilization and crosslinking of acrylated AG; [d]AG–HEP-grafted silicone prepared by UV-induced immobilization and crosslinking of acrylated AG and methacrylated HEP; [e]HEP-grafted silicone prepared by UV-induced immobilization and crosslinking of methacrylated HEP.

to attach to hydrophobic surfaces due to hydrophobic interactions.[21] Thus, the ability of the AG, AG–HEP, and HEP modified silicone to inhibit *S. aureus* adherence can be attributed to the improved surface hydrophilicity which results from the grafting of the hydrophilic polymers. Since it has been reported that some adhered bacteria may be washed off the surface during washing procedures due to forces at the air-liquid interface, the number of bacteria on the films (as shown in Figure 4) may reflect bacterial retention rather than bacterial adhesion per se.[48]

The anti-adhesive property of the AG, AG–HEP, and HEP modified silicone can be further illustrated by the fluorescence microscopy images of adherent *S. aureus* cells on pristine and modified silicone films (Figure S2). Large number of viable *S. aureus* (stained green with SYTO 9) can be observed on pristine silicone film (Figure S2(a)). On the AG, AG–HEP, and HEP modified silicone surfaces, the number of viable bacteria was significantly reduced (Figure S2(b–d)). Very few dead or membrane-compromised bacteria (stained red with propidium iodide (PI)) can be observed on all the silicone surfaces (Figure S2(a'–d')). Thus, the AG and HEP polymers are anti-adhesive, but not bactericidal. The anti-adhesive property of the AG-modified silicone strongly depends on the grafting density of the immobilized AG layer, which is associated with the UV-induced grafting time (Figure S3). The efficacy in inhibiting *S. aureus* and *E. coli* adhesion increases with the increasing UV irradiation time. After 120 min of UV induced grafting, the resulting Silicone-*g*-AG4 reduced *S. aureus* and *E. coli* adhesion by ~98% and ~99%, respectively.

HEP is less effective in reducing *S. aureus* adhesion than AG (comparing Figure 4(d) with 4(b)). Thus, the grafting of a large amount of HEP on AG–HEP-modified silicone will result in an increase in the number of adherent bacteria. If the surface concentration of immobilized HEP is restricted to 2.6 μg cm^{-2} or less, the antibacterial efficacy of Silicone-*g*-AG-HEP will not be significantly different from that of Silicone-*g*-AG4 (comparing the number of adherent bacteria on the Silicone-*g*-AG-HEP films with different surface concentrations of HEP in Figure S4).

Bacterial biofilms are the major cause of peritonitis and other PD catheter-related infections in PD.[49] In this work, the efficacy of the polymer-modified silicone films in inhibiting biofilm formation was assessed after incubation in growth medium containing 10^7 bacterial cells mL^{-1} for 48 h. **Figure 5** shows the SEM images of bacterial biofilm on pristine and modified silicone surfaces. It can be seen from Figure 5(a) and (d) that both *S. aureus* and *E. coli* readily form a thick biofilm on the pristine silicone film. After surface grafting of AG on the silicone surface, significant reduction in bacterial biofilm was observed. There is no obvious *S. aureus* biofilm but some bacterial clusters are present on the Silicone-*g*-AG4 and Silicone-*g*-AG-HEP1 films (Figure 5(b) and (c), respectively). The Silicone-*g*-AG4 and Silicone-*g*-AG-HEP1 films are even more effective in preventing *E. coli* biofilm formation, and only a few individual bacterial cells can be observed (Figure 5(e) and (f), respectively). These results suggest that *S. aureus* biofilm formation on silicone surface is more difficult to prevent than *E. coli* biofilm, which is consistent with a previous report.[50] Nevertheless, quantification of the number of adherent bacteria on pristine and modified silicone films showed that the modified silicone (Silicone-*g*-AG4 and Silicone-*g*-AG-HEP1) reduced the number of adherent *S. aureus* and *E. coli* by ~2.4 and ~3.3 orders of magnitude, respectively (**Figure 6**(a) and (b)), compared to the pristine film. In addition to *E. coli* and *S. aureus*, *P. aeruginosa* (Gram-negative) biofilm formation on the AG and AG–HEP modified silicone films was also assessed since *P. aeruginosa* is another major cause of infection in PD dialysis.[5] The number of adherent *P. aeruginosa* cells on the AG and AG–HEP modified films was reduced by more than 2 orders of magnitude compared to pristine silicone (Figure S5). Thus, the bacterial adhesion and biofilm formation assays indicate that the AG and AG–HEP graft layers are effective against *E. coli*, *S. aureus* and *P. aeruginosa* bacterial species.

In addition to the flat silicone film surface, the AG and AG-HEP polymer were grafted onto tubular PD catheter surface via ozone treatment followed by heat-induced immobilization and crosslinking of the polymer layer. By changing the heating period, the thickness of the AG graft layer can be

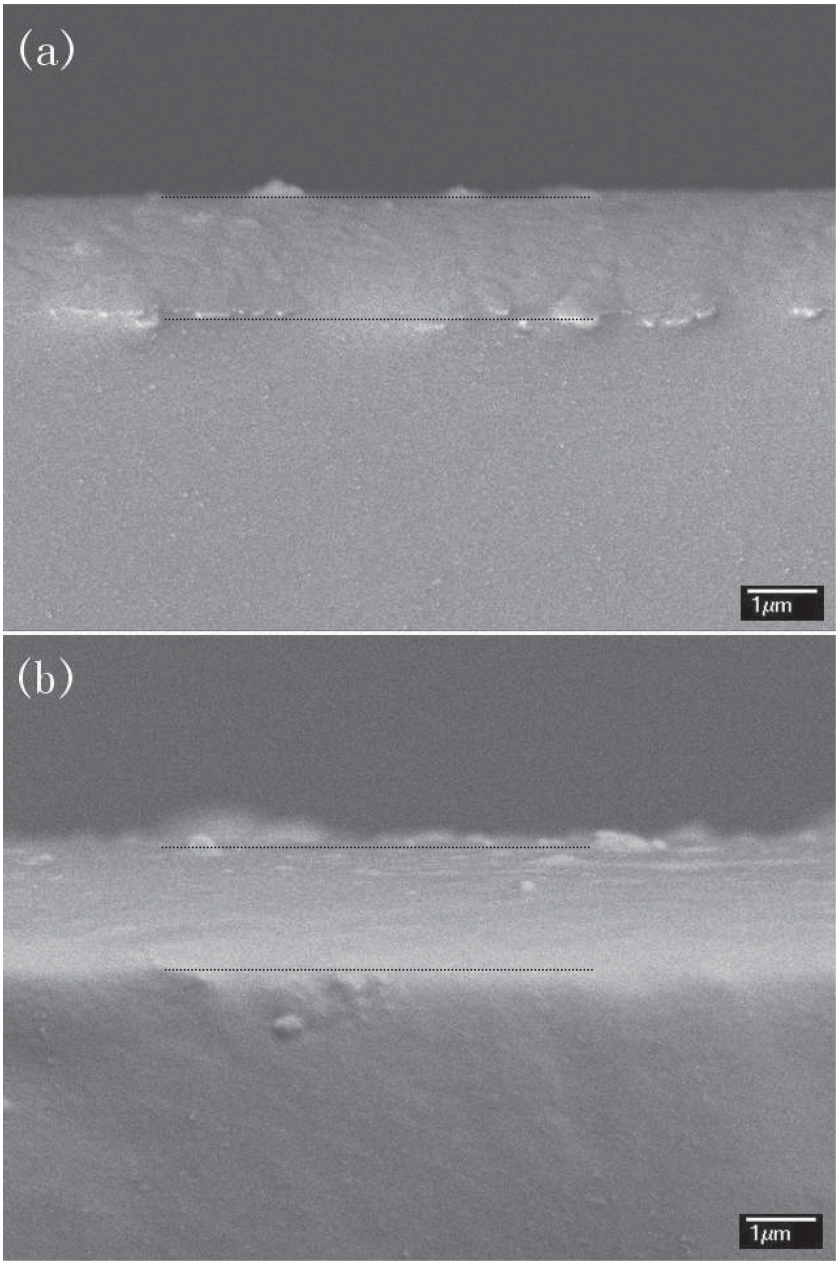

Figure 3. FESEM images of the cross-section of a) Silicone-*g*-AG4 and b) Silicone-*g*-AG-HEP1 films. Scale bar is 1 μm.

varied. This is illustrated in Figure S6(a) and S6(b), which show the cross-section of AG-modified PD catheter prepared using a heating period of 8 h and 18 h, respectively. These heating periods resulted in an AG graft layer of ~2 and ~5 μm thickness, respectively. Figure S6(c) shows the number of adherent *E. coli* cells on the pristine and modified catheter surfaces after 48 h of incubation in culture medium. The AG and AG-HEP modified PD catheters reduced the number of adherent bacterial cells by more than 3 orders of magnitude, similar to the results obtained with the Silicone-*g*-AG4 film. In addition, no significant difference in the number of adherent bacterial cells was found on the modified catheters with 2 μm and 5 μm of polymer graft layer, indicating that there is no substantial improvement in the antibacterial efficacy of the AG and AG-HEP coatings of thickness beyond 2 μm.

2.3. Stability

The stability of coatings applied on PD catheters is a crucial requirement since PD catheters need to be placed in the abdomen for a long time. The stability of the AG and AG–HEP modified silicone films was assessed by conducting the bacterial biofilm assay and the contact angle measurement on the films after they were aged in lysozyme solution at 37 °C for 30 days. As shown in Figure 6(a), the number of adherent *S. aureus* after the biofilm assay increased slightly but not significantly ($P>0.05$) on the aged AG and AG–HEP modified films. Similar results were also obtained for *E. coli* (Figure 6(b)). The contact angles of the aged Silicone-*g*-AG4 and Silicone-*g*-AG-HEP1 films were 32° and 30°, respectively, which are not significantly different from the values before aging (30° and 29°, respectively). In addition, the biofilm formation assay also shows that the Silicone-*g*-AG4 and Silicone-*g*-AG-HEP1 films maintain their antibacterial property after autoclaving at 121 °C for 20 min (Figure 6(a) and (b)). These results suggest that the crosslinked AG and AG–HEP layers on silicone are stable. The stability of the graft layer after aging for 30 days also indicates that the crosslinked AG and AG–HEP layers are able to prevent the hydrophobic recovery of silicone and retain their antibacterial efficacy.

A similar aging experiment in the lysozyme solution for 30 days was carried out with crosslinked AG and AG–HEP hydrogels and uncrosslinked AG hydrogel. For the crosslinked AG and AG–HEP hydrogels, a weight loss of 13.5% and 11.8%, respectively, was observed. The uncrosslinked AG hydrogel showed a higher weight loss of 22.7%, which corresponds well to the degradation of uncrosslinked AG hydrogel in vivo in a previous study.[51] Biofilm assay carried out with aged Silicone-*c*-AG film (uncrosslinked AG coated silicone film) (Figure 6) also confirmed that the uncrosslinked AG coating is not as stable in lysozyme solution as the crosslinked one. In addition, the Silicone-*c*-AG film after autoclaving at 121 °C for 20 min does not possess antibacterial property since the uncrosslinked AG layer was only physically adsorbed on the film and it melted away during autoclaving.

When a PD catheter is inserted into the body, it will encounter frictional and bending forces. The stability of the crosslinked AG and AG–HEP layer on catheter after being

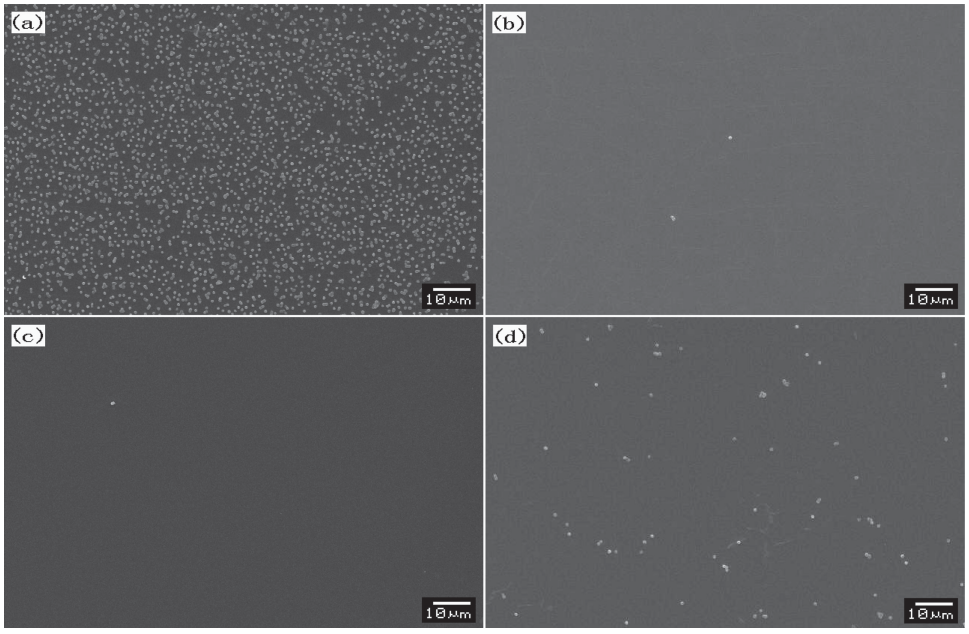

Figure 4. SEM images of a) pristine silicone, b) Silicone-*g*-AG4, c) Silicone-*g*-AG-HEP1, and d) Silicone-*g*-HEP film surfaces after exposure to a PBS suspension of *S. aureus* (10^8 cells mL^{-1}) for 4 h. Scale bar is 10 μm.

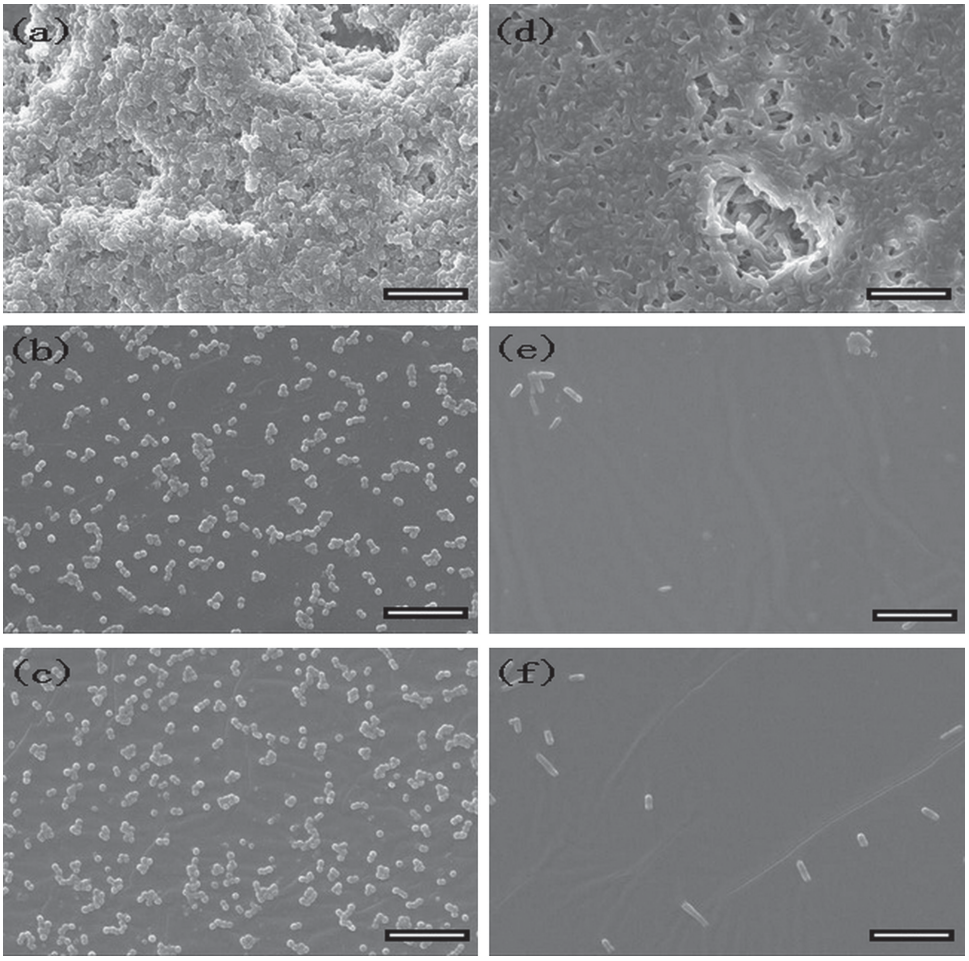

Figure 5. SEM images of a–c) *S. aureus* and d–f) *E. coli* biofilm on a,d) pristine, b,e) Silicone-*g*-AG4 and c,f) Silicone-*g*-AG-HEP1 films after incubation in growth medium containing 10^7 bacterial cells mL^{-1} for 48 h. Scale bar is 10 μm.

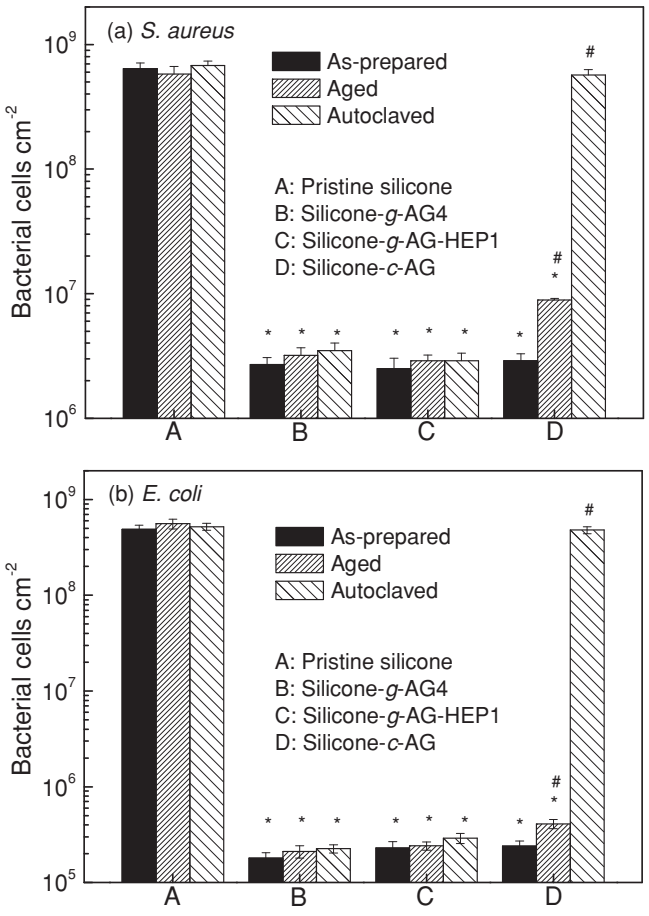

Figure 6. Quantitative count of adherent a) *S. aureus* and b) *E. coli* cells per cm^2 of the pristine and modified film surfaces after incubation in growth medium containing 10^7 bacterial cells mL^{-1} for 48 h as determined by the spread plate method. * Significant differences ($P < 0.05$) compared with pristine silicone. # Significant differences ($P < 0.05$) compared with respective as-prepared film.

subjected to such forces was evaluated using the bacterial biofilm formation assay and the results are shown in Figure S7. The AG and AG–HEP modified catheters showed good stability since there is no significant change in the number of adherent bacteria on the modified catheter after the friction and bending tests.

2.4. Protein Adsorption and Cell Adhesion

Omental wrapping is the leading cause of outflow failure in PD treatment. The omentum is the primary peritoneal defense organ, and in response to inflammation or foreign matter, it will adhere to and wall off the affected area. Protein adsorption on the surface of PD catheter is a crucial factor for omental wrapping since the mechanism for omental adhesion is believed to involve the formation of fibrin exudates at the site of insult, which attracts active migration of fibroblasts and leukocytes and finally leads to encapsulation of the affected area.[52] In this work, the adsorption of two kinds of proteins, FBG and BSA, on the modified silicone films was investigated.

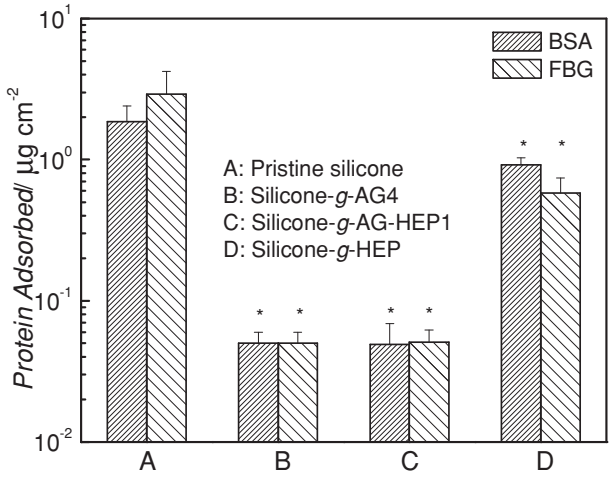

Figure 7. BSA and FBG adsorption on pristine silicone, Silicone-*g*-AG4, Silicone-*g*-AG-HEP1 and Silicone-*g*-HEP films after the films were treated with 1.0 mg mL^{-1} of pure protein solutions for 4 h. *Significant differences ($P<0.05$) compared with pristine silicone.

As shown in **Figure 7**, the amount of adsorbed FBG and BSA on pristine silicone film is ~2.9 and ~1.9 μg cm^{-2}, respectively. After grafting with AG, the protein adsorption was very significantly reduced. The Silicone-*g*-AG4 film reduced BSA and FBG adsorption by ~98%, and the Silicone-*g*-AG-HEP1 film showed a similar reduction of protein adsorption. Non-specific adsorption of proteins on the hydrophilic AG polymer is known to be very low, and AG and its derivatives are often used as the supporting materials for protein separation to minimize the non-specific adsorption.[53] Thus, the observed reduction in protein adsorption on the Silicone-*g*-AG4 and Silicone-*g*-AG-HEP1 films can be attributed to the AG layer. On the other hand, the Silicone-*g*-HEP film is less effective in reducing protein adsorption (adsorbed BSA and FBG was reduced by ~51% and ~80%, respectively). This is because HEP is able to interact with some kinds of proteins, including BSA and FBG.[54,55] Nevertheless, if the immobilized HEP is low (2.6 μg cm^{-2}), such as on the Silicone-*g*-AG-HEP1 film, the protein-repellent property of AG is preserved (compared with the Silicone-*g*-AG4, Figure 7).

The effect of protein adsorption on pristine silicone and Silicone-*g*-AG4 films on subsequent bacterial adhesion and biofilm formation was investigated using FBG and *S. aureus*. Figure S8(a) and S8(b) show the SEM images of adherent *S. aureus* on these films after pretreatment with FBG. Increased clustering of the bacterial cells can be observed in Figure S8(a) as compared with Figure 4(a), which is consistent with results reported earlier that showed pre-adsorbed FBG on polypyrrole surface enhances *S. aureus* adhesion on the surface and clumping.[56] This is attributed to the FBG binding protein (clumping factor) expressed by the *S. aureus* cells.[57] The number of adherent bacterial cells increased slightly on the Silicone-*g*-AG4 film after pretreatment with FBG (comparing Figure S8(b) with 4(b)) but these cells remained as single units rather than clusters. Figure S8(c) and S8(d) show the SEM images of *S. aureus* biofilm on the pristine silicone and Silicone-*g*-AG4 films pre-treated with FBG. A thick biofilm formed

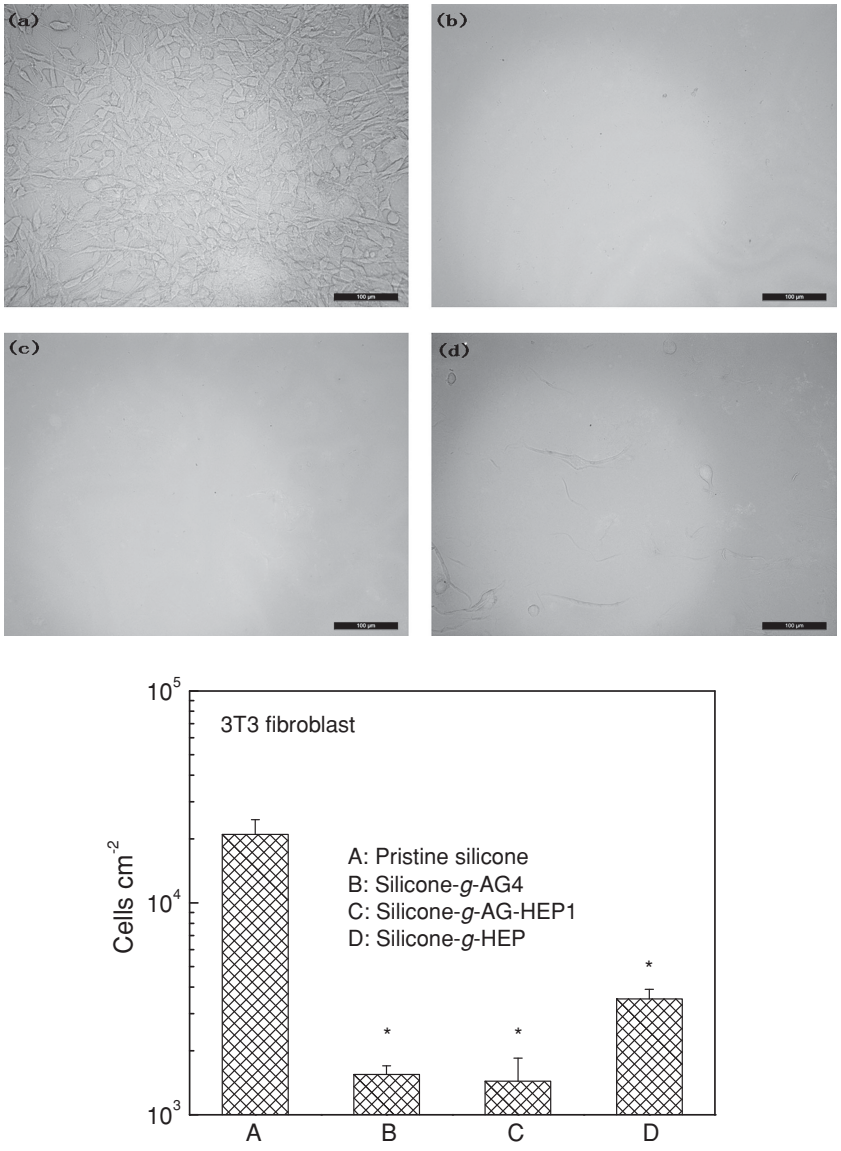

Figure 8. Optical microscopy images of a) pristine silicone, b) Silicone-*g*-AG4, c) Silicone-*g*-AG-HEP1, and d) Silicone-*g*-HEP film surfaces after incubation with 3T3 fibroblasts (2×10^5 cells mL^{-1}) for 24 h. Scale bar is 100 µm. e) Quantitative analysis of adherent 3T3 fibroblast cells per cm^2 of film surface using MTT assay. * Significant differences ($P<0.05$) compared with pristine silicone.

on pristine silicone film regardless of whether FBG is present or not. However, the Silicone-*g*-AG4 film after FBG pretreatment is still able to resist biofilm formation because the extent of FBG adsorption is low (Figure 7).

In the cell adhesion assay, 3T3 mouse fibroblasts were selected as model mammalian cells to study their interaction with the modified silicone films. **Figure 8**(a–c) show the optical microscopy images of the adherent 3T3 fibroblast cells on the pristine and modified silicone surfaces. A large number of 3T3 fibroblasts readily adhered, spread and grew very well on the pristine silicone surface (Figure 8(a) and S9), while fibroblast adhesion was almost completely inhibited on the AG and AG–HEP modified surfaces (Figure 8(b) and 8(c)). It can also be seen from Figure 8(d) that HEP is not as effective in preventing 3T3 fibroblast adhesion as AG and AG–HEP. The AG and AG–HEP modified silicone reduced 3T3 fibroblast adhesion by ~92% and ~93%, respectively, as compared to pristine silicone, while the reduction on the HEP modified silicone is ~83% (Figure 8(e)). The difference in the extent of fibroblast cell adhesion on the AG, AG–HEP, and HEP modified silicone films is likely related to their protein-repellent properties, as it has been reported that reduction of non-specific protein adsorption is critical in the inhibition of cellular interaction with material surface.[58]

Although AG and HEP are known to be nontoxic, the cytotoxicity of the modified silicone films need to be tested since the as-prepared AG and AG–HEP coatings are meant for implantable devices. The cytotoxicity of the pristine and modified silicone films was evaluated with 3T3 fibroblasts using the MTT assay. The viability of 3T3 fibroblasts placed in contact with the pristine and modified films for 24 h was higher than 95% in all cases (Figure S10). No significant difference in the cell viabilities was found as compared to that in the control experiment (without any film present), indicating that these films possess no or very low cytotoxicity. These cell viability results also confirm that the reduction of cell adhesion on the modified silicone surfaces (Figure 8) is due to the anti-adhesive property of the polymer coatings and not because of their cytotoxicity.

2.5. Hemocompatibility Assays

Hemocompatibility is an important property for biomedical devices in contact with blood in human body. In PD, blood clotting and thrombosis induced by platelet adhesion and activation can result in intraluminal obstruction and eventual outflow failure of PD catheters.[7] The blood compatibility of the AG and AG–HEP modified silicone films was evaluated from platelet adhesion and activation, hemolysis and plasma recalcification time (PRT) tests. The SEM images of platelet adhesion on pristine and modified silicone films are shown in **Figure 9**(a–d). Platelets adhered readily on pristine silicone surface (Figure 9(a)) and the adherent platelets were highly activated with the characteristics of pseudopodia and spreading. After the grafting of AG and AG–HEP on silicone, the number of adherent platelets significantly decreased (Figure 9(b) and (c)). The quantitative comparison of the number of adherent platelets on various films (Figure 9(e)) shows that platelet adhesion on the modified silicone surface was reduced by more than 1 order of magnitude as compared to the pristine surface.

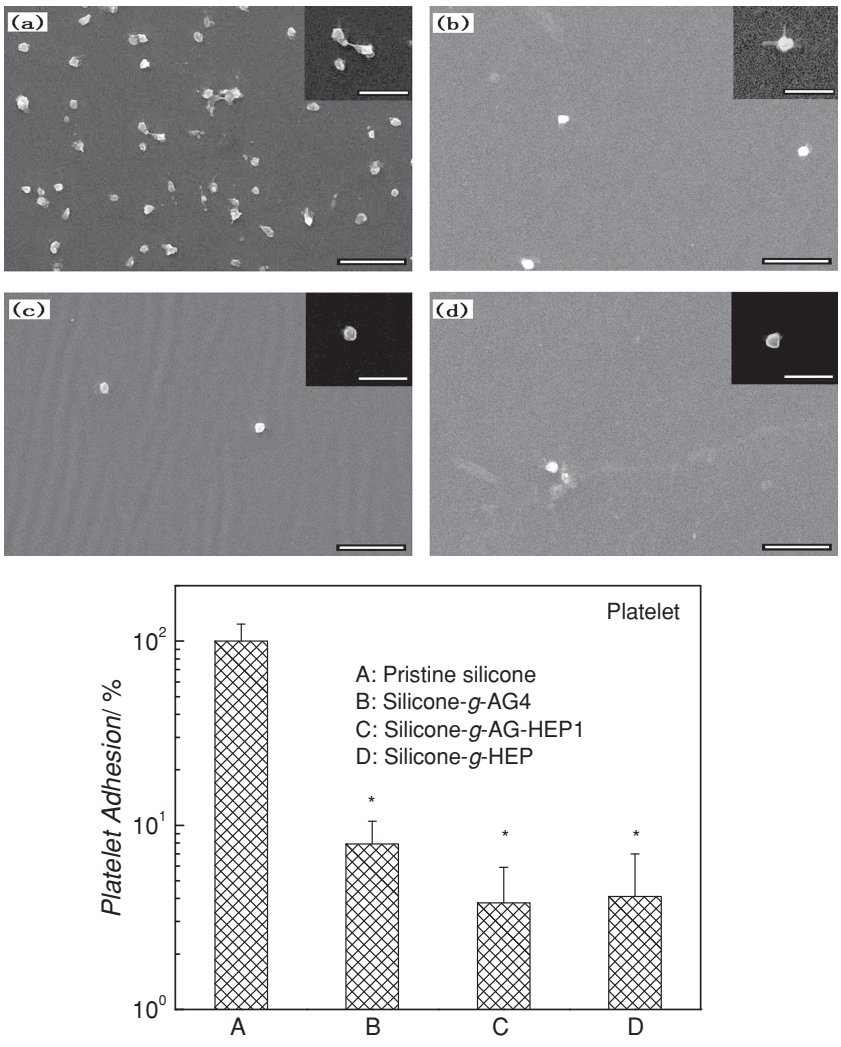

Figure 9. SEM images of a) pristine silicone, b) Silicone-*g*-AG4, c) Silicone-*g*-AG-HEP1, and d) Silicone-*g*-HEP film surfaces after incubation with platelet-rich plasma for 1 h. Scale bar in (a–d) and their insets is 10 and 5 μm, respectively. e) Platelet adhesion on the modified silicone surfaces relative to that on the pristine surface. * Significant differences ($P < 0.05$) compared with pristine silicone.

The resistance to platelet adhesion on the AG and AG–HEP modified silicone films is again attributed to their protein-repellent property as discussed above since plasma protein adsorption, in particular the adsorption of platelet adhesion promoting protein, FBG, plays an important role in platelet adhesion on biomaterial surfaces.[59] However, it should be noted that the platelets on the Silicone-*g*-AG4 film are still activated (inset of Figure 9(b)), indicating that the AG coating is not effective in inhibiting the activation of platelets. On the other hand, the AG–HEP coating is effective in preventing activation of the platelets (inset of Figure 9(c)), and this can be ascribed to the presence of HEP in the AG–HEP layer. HEP is commonly used as an anticoagulant agent and has been reported to be able to inhibit platelet adhesion and activation,[60] which is confirmed by the low degree of platelet adhesion and activation on the Silicone-*g*-HEP film (Figure 9(d)).

Figure 10(a) shows the PRT results obtained from the blood clotting tests on the pristine and modified silicone films. Grafting of AG on silicone resulted in a significant increase in PRT from ~13 to ~16 min ($P<0.05$), and with the presence of HEP in the AG graft layer, the PRT increased further to ~19 min. HEP is known to bind to antithrombin III (ATIII) with high affinity, resulting in a conformational change of ATIII. With this conformational change, ATIII's reactive sites are more exposed, which greatly accelerates ATIII's inhibition of the activity of blood coagulation proteases, and consequently delays the conversion of fibrinogen to fibrin and inhibits blood coagulation.[61] Hemolysis is another issue related to the hemocompatibility of biomaterials in contact with blood. Figure 10(b) shows the degree of hemolysis obtained with the pristine and modified silicone films. The degree of hemolysis of pristine silicone was ~1%. After the grafting of AG, AG-HEP and HEP, the modified silicone films showed significantly lower hemolysis degrees ($P < 0.05$), ranging from 0.77% for the Silicone-*g*-AG4 to 0.56% for the Silicone-*g*-HEP film. Although according to the American Society for Testing and Materials (ASTM) F 756–00 standard,[62] a hemolysis degree of 2% is considered nonhemolytic for biomaterials and the pristine silicone meets this requirement, the modified films further reduced the degree of hemolysis and subsequently improved the silicone's hemocompatibility.

3. Conclusion

AG and HEP polymers were covalently immobilized on medical grade silicone film and silicone PD catheter surfaces to improve their antibacterial, antifouling and hemocompatible properties. The adhesion and biofilm formation of *E. coli*, *P. aeruginosa* (both Gram-negative) and *S. aureus* (Gram-positive) bacteria were reduced by > 2 orders of magnitude on the AG-modified surface as compared to that on pristine silicone. The crosslinked AG coating of ~2 μm thickness is stable and maintains its antibacterial efficacy after 30 days aging in lysozyme solution and also after autoclaving. In addition, the AG coating can effectively resist non-specific protein adsorption and fibroblast and platelet adhesion. Co-immobilization of 2.6 μg cm^{-2} of HEP in the AG coating further improves hemocompatibility by inhibiting platelet activation, prolonging PRT and reducing the degree of hemolysis. Concomitantly, the antibacterial and antifouling efficacy of AG is retained. The favorable antibacterial, antifouling and improved hemocompatible properties as well as non-cytotoxicity of the modified silicone offer promising

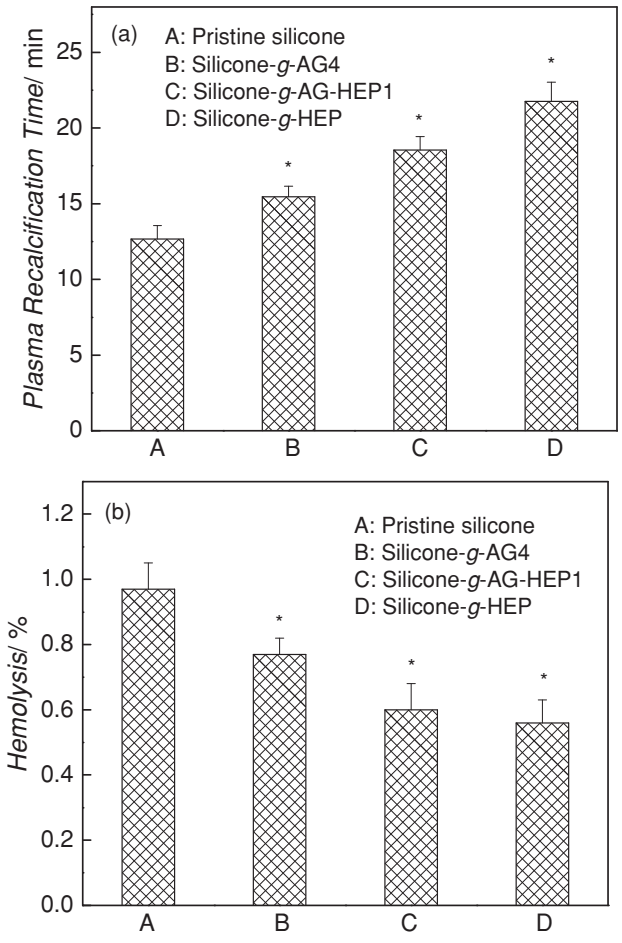

Figure 10. a) PRT and b) degree of hemolysis on pristine silicone, Silicone-*g*-AG4, Silicone-*g*-AG-HEP1 and Silicone-*g*-HEP film surfaces. * Significant differences ($P < 0.05$) compared with pristine silicone.

opportunities for combating infection and omental wrapping of PD catheters.

4. Experimental Section

Materials: Medical grade silicone films were purchased from Bioplexus Inc. (Ventura, CA, USA). Quinton silicone peritoneal dialysis (PD) catheters were purchased from Tyco International Ltd. (Princeton, NJ, USA). Agarose (AG) was purchased from Bio-Rad Laboratories (Hercules, CA, USA). Sodium heparin (HEP) and 3-[4,5-dimethyl-thiazol-2-yl]-2,5-diphenyltetrazolium bromide (MTT) were purchased from Alfa Aesar Co. (Ward Hill, MA, USA). Acryloyl chloride (97%), methacrylic anhydride (94%), bovine serum albumin (BSA), bovine plasma fibrinogen (FBG) and all solvents used (analytical grade) were purchased from Sigma–Aldrich (St. Louis, MO, USA). *Escherichia coli* (*E. coli*, ATCC DH5α), *Staphylococcus aureus* (*S. aureus*, ATCC 25923) and 3T3 mouse fibroblast cells were purchased from American Type Culture Collection (Manassas, VA, USA). *Pseudomonas aeruginosa* (*P. aeruginosa*, PAO1) was purchased from National Collection of Industrial Food and Marine Bacteria (NCIMB, Bucksburn, Aberdeen, Scotland). The acrylated AG was prepared using similar procedures described in the literature.[63] Briefly, AG (1.0 g) was dissolved in *N*,*N*-dimethylacetamide (DMAC, 25 mL) at 100 °C. After AG was dissolved completely, the solution was cooled to 0 °C in an ice-water bath. Then, acryloyl chloride (0.125 mL) in DMAC (2.5 mL) was added dropwise into the AG solution with stirring. The reaction was allowed to proceed for 1 h at 0 °C and for another 4 h at 25 °C. The acrylated AG product was precipitated in an excess volume of acetone and washed thoroughly with acetone followed by drying under reduced pressure. The methacrylated HEP was prepared using a procedure similar to that described in the literature.[64] HEP (200 mg) were dissolved in doubly distilled water (10 mL). Then, methacrylic anhydride (10 µL) was added in the solution, and the pH of the solution was adjusted to 8.5 using 4 M NaOH solution. The solution was left to react overnight at 0 °C with stirring. The methacrylated HEP product was precipitated in an excess volume of cold ethanol followed by dialysis against water for 72 h using a dialysis tubing (molecular weight cut-off of 1000, Spectrum Laboratories Inc., Rancho Dominguez, CA, USA). The methacrylated HEP solution was freeze-dried after dialysis.

Preparation of AG, HEP, and AG–HEP Grafted Silicone Films and Catheters: For the preparation of crosslinked AG grafted silicone films (Silicone-*g*-AG), medical grade silicone film was cut into 2 × 2 cm^2 pieces and ultrasonically cleaned in isopropanol, ethanol and doubly distilled water for 10 min in each step. The clean silicone films were subjected to oxygen plasma for 5 min in an Anatech SP100 plasma system. The oxygen plasma treated films were then exposed to the atmosphere for another 10 min to promote the formation of peroxide groups on the plasma-treated surfaces. These peroxide groups served as active sites to initiate the subsequent UV-induced immobilization and crosslinking reaction for grafting acrylated AG onto the oxidized surfaces. Acrylated AG aqueous solution (5 wt%, 200 µL) were dropped onto the surface of the plasma-treated silicone film which was placed on a SCS P6206 spincoater. Spin-coating was carried out at a speed of 1000 rpm for 60 s. The procedure was then repeated for the other surface of the film. The silicone film with spin-coated acrylated AG was then placed in a Pyrex glass tube and degassed with argon for 30 min. The glass tube was sealed and irradiated with UV light in a Riko rotary photochemical reactor (Model RH400–10W) for 15, 30, 60 and 120 min to obtain the Silicone-*g*-AG1, Silicone-*g*-AG2, Silicone-*g*-AG3 and Silicone-*g*-AG4 films (Table 1), respectively. After irradiation, the Silicone-*g*-AG films were washed thoroughly with doubly distilled water at 60 °C for 24 h to remove the physically adsorbed acrylated AG. After washing, the modified silicone film was stored in doubly distilled water prior to use (usually ~24–48 h). The HEP modified silicone films (Silicone-*g*-HEP) and AG-HEP modified silicone films (Silicone-*g*-AG-HEP) were similarly prepared using the methacrylated HEP solution, and a mixture of acrylated AG and methacrylated HEP solutions with different ratios as indicated in Table 1, respectively. The uncrosslinked AG coated silicone films (Silicone-*c*-AG) were similarly prepared using the unmodified AG solution. The concentration of acrylated AG, methacrylated HEP and unmodified AG in the solutions used was fixed at 5 wt%.

For the preparation of AG and AG–HEP grafted silicone catheter, the catheter was cut into 6 cm segments and washed with isopropanol, ethanol and water as described above. The oxygen plasma pretreatment and spin coating method employed for grafting AG or AG–HEP on silicone films are not appropriate for catheters since both the extraluminal and intraluminal surfaces of the catheter have to be modified. In order to activate both the extraluminal and intraluminal surfaces of the catheter segments, ozone was used instead. After pretreatment with an oxygen-ozone gas mixture (generated from an Azcozon ozone generator (Model VMUS-4PSE) at an oxygen inlet flow rate of 60 L h^{-1}, and ozone production rate of about 3.6 g h^{-1}.) for 20 min, the ozone-treated catheter segment was introduced into a Pyrex glass tube containing the respective reagent (5 wt.%) as described above and degassed with argon for 30 min. The glass tube was sealed and heated to and then maintained at 70 °C in an oil bath for 8 h. After the reaction, the AG or AG–HEP modified catheter segment was washed with doubly distilled water at 60 °C for 24 h. After washing, the modified silicone catheter segment was stored in doubly distilled water prior to use (usually ~24–48 h).

Crosslinked AG hydrogel (without silicone film) was prepared by adding 4,4′-azobis(4-cyanovaleric acid) (5 mg) to a Pyrex tube containing acrylated AG aqueous solution (5 wt%, 10 mL). After purging with argon for 30 min, the flask was sealed and irradiated with UV light

in a Riko rotary photochemical reactor for 120 min. After irradiation, the crosslinked AG hydrogel was washed with ethanol and doubly distilled water at 60 °C for 24 h followed by freeze-drying. Crosslinked AG–HEP hydrogel was similarly prepared using a mixture of acrylated AG and methacrylated HEP solution (acrylated AG: methacrylated HEP = 9:1 (w/w)). Uncrosslinked AG gel was prepared by heating the unmodified AG solution to 120 °C and cooled to 25 °C followed by freeze-drying.

Bacterial Adhesion and Biofilm Formation Assay: Bacteria were cultured overnight in growth medium (tryptic soy broth for *S. aureus*, nutrient broth for *E. coli* and lysogeny broth for *P. aeruginosa*). The bacteria-containing growth broth was then centrifuged at 2700 rpm for 10 min to remove the supernatant. The bacterial cells were washed with PBS (pH 7.4) and resuspended in PBS at a concentration of 10^8 cells mL^{-1}, as estimated from optical density (OD) at 540 nm (OD of 0.1 at 540 nm is equivalent to ~10^8 cells mL^{-1} based on spread plate counting). The pristine and modified silicone films of size 1×1 cm^2 were placed in a 24-well plate and covered with bacterial suspension (1 mL) at 37 °C for 4 h. After the bacterial adhesion process, the films were washed thrice with PBS to remove the non-adherent bacteria. For the quantification of adherent bacteria, the spread plate method was carried out as described in the literature.[65,66] Briefly, the films with adherent bacteria were put into PBS (2 mL) and ultrasonicated for 7 min (using a 100 W sonicator) followed by vortexing for 30 s to release the bacterial cells into the PBS.[67] The bacterial suspension was serially diluted and spread on an agar plate. After culturing overnight, the number of viable bacterial cells was quantified by counting the number of colonies on the agar plate. For SEM observation, the adherent bacteria on the films were fixed with 3 vol% glutaraldehyde in PBS overnight at 4 °C. After serial dehydration with 25%, 50%, 75%, and 100% ethanol for 10 min each, the films were dried under reduced pressure, coated with platinum, and observed under SEM. For the assessment of the viability of adherent bacteria on pristine and modified silicone, the films were stained by a combination dye (LIVE/DEAD *Bac*Light Bacterial Viability Kit) and observed under a Leica DMLM microscope equipped with a 100 W Hg lamp.

For the assessment of biofilm formation by *S. aureus*, *E. coli*, and *P. aeruginosa*, overnight bacterial culture broth was diluted to a concentration of 10^7 cells mL^{-1} with their respective growth medium. The pristine and modified silicone substrates (1×1 cm^2 films or 1 cm catheter segments) were placed in a 24-well plate and covered by bacterial suspension (1 mL) at 37 °C for 48 h to allow biofilm growth. The growth medium was replaced with a fresh one after 24 h. After the biofilm growth period, the substrates were washed thrice with PBS. The films were observed under SEM, and the number of biofilm bacterial cells on the films and catheter segments (both intraluminal and extraluminal surfaces) was quantified using the spread plate method as described above.

Stability Tests: The stability of the AG and AG–HEP graft layer on the silicone films was assessed by aging the films in lysozyme aqueous solution (10 μg mL^{-1}) for 30 days at 37 °C. The lysozyme concentration was selected to simulate its concentration in human serum.[68] After the aging period, assessment of bacterial biofilm formation on the films was carried out as described above to test the stability of the coating. For comparison purposes, the degradation of as-prepared AG and AG–HEP hydrogels (without silicone film) in lysozyme solution was also carried out. The dry AG and AG–HEP hydrogels (100 mg for each) were aged in lysozyme solution (10 μg mL^{-1}, 10 mL) for 30 days at 37 °C. After the aging period, the hydrogel was dialyzed against water for 72 h using a dialysis tubing (molecular weight cut-off of 3500, Spectrum Laboratories Inc., Rancho Dominguez, CA, USA) followed by freeze-drying. The degree of weight loss (WL) was calculated as follows:

$$WL = (WB - WA)/WB \times 100\% \quad (1)$$

where WB and WA are the weight of hydrogel before and after aging, respectively.

The stability of the modified PD catheter under frictional forces was carried out by pulling the catheter segments between two pieces of raw meat (pork). The meat was fixed between two poly(methyl methacrylate) plates of length of 5 cm. A modified catheter segment of 6 cm length was inserted between the two pieces of meat from one side and pulled out from the other side. This procedure was repeated 5 times. After the friction test, the catheter segment was cut into 1 cm length and assay of bacterial biofilm formation on the catheter segment was carried out as described above to test the stability of the grafted layer. The 6 cm modified catheter segments were also subjected to bending tests whereby the segment was bent into a circle upwards and downwards 15 times. After the bending test, the middle 3 cm of the catheter, which was subjected to the highest bending stress, was cut into three segments of 1 cm length, and assay of bacterial biofilm formation on the these segments was then carried out.

Protein Adsorption: Pristine and modified silicone films of size 2 × 2 cm^2 were first equilibrated for 1 h in CPBS (citrate-phosphate buffer saline, PBS and 0.01 M sodium citrate, pH 7.4), and then immersed in pure BSA or FBG protein solution (1.0 mg mL^{-1} in CPBS) for 4 h at 37 °C. After this protein adsorption period, the films were washed with CPBS and doubly distilled water twice, respectively. The modified dye-interaction method using Bio-Rad protein dye reagent (Catalog No. 500–0006) was employed to determine the amount of adsorbed protein on the films. The procedure used was similar to that described in the literature.[69] Briefly, protein solutions (0.4 mL) of different known concentrations were added to the 5-time diluted stock dye solution (10 mL). After 10 min, centrifugation was carried out at 5000 rpm for 15 min, and the absorbance of the supernatant of the protein-dye solutions at 465 nm was used to obtain a standard calibration curve. For the quantification of adsorbed protein on the film, the film was put in the dye solution (10 mL). After 3 h of immersion, the film was removed. The remaining solution was centrifuged and the absorbance of the supernatant was measured at 465 nm. The amount of adsorbed protein on the films was calculated from the standard calibration curve. A control experiment was carried out to confirm that heparin would not interact with the dye.

To determine the effect of pre-adsorbed protein on bacterial adhesion and biofilm formation, *S. aureus* adhesion and biofilm formation on the pristine and AG-modified silicone films after these films were pre-treated with FBG protein for 4 h at 37 °C were investigated using the procedures described above.

Cytotoxicity Assay: The cytotoxicity of the modified silicone films was investigated using the standard MTT assay. DMEM supplemented with 10% fetal bovine serum, 1 mM L-glutamine, 100 IU mL^{-1} penicillin was used to culture 3T3 fibroblast cells. One mL medium containing the DMEM 3T3 fibroblasts at a density of 10^4 cells mL^{-1} were placed in each well of a 24-well plate. The plate was then incubated in a humidified atmosphere of 95% air and 5% CO_2 at 37 °C for 24 h. After replacing the medium with a fresh one, the films of size 1 × 1 cm^2 were gently placed on top of the cell layer in the well. The control experiment was carried out using the complete growth culture medium without the film (nontoxic control). After incubation for another 24 h at 37 °C, the culture medium and film in each well was removed. Culture medium (900 μL) and MTT solution (5 mg mL^{-1} in PBS, 100 μL) were then added to each well. After 4 h of incubation, the MTT solution and medium was removed and dimethyl sulfoxide (DMSO, 1 mL) was added to dissolve the formazan crystals. The optical absorbance at 570 nm was then measured on a Bio-Tek microplate reader (Model Powerwave XS). The results were expressed as percentages relative to the optical absorbance obtained in the control experiment.

Cell Adhesion: Pristine and modified silicone films of size 1 × 1 cm^2 were placed in a 24-well plate. Culture medium (1 mL) containing 3T3 fibroblasts at a density of 2 × 10^5 cells mL^{-1} was added and incubated for 24 h. After the incubation period, the films were rinsed thrice with medium to remove non-adherent cells. The film surfaces with adherent cells were viewed using a Leica DMLM microscope. For quantification of adherent 3T3 fibroblast cells, the films with adherent cells were placed in a 24-well plate and MTT assay was carried out. A standard calibration curve was generated by seeding a known number of 3T3 fibroblast cells in a 24-well plate and incubating for 4 h at 37 °C followed by MTT assay. The number of 3T3 fibroblasts adhered on the films was calculated from the standard calibration curve.

Platelet Adhesion: Fresh blood collected from a healthy rabbit was immediately mixed with 3.8 wt% sodium citrate solution in a ratio of

9:1 (v/v). Platelet-rich plasma (PRP) was obtained by centrifuging the blood at 700 rpm and 8 °C for 10 min. The PRP was diluted with PBS in a ratio of 1:1 (v/v), and the diluted PRP (0.1 mL) was introduced on the surface of a 1 × 1 cm^2 silicone film. After incubation at 37 °C for 1 h, the film was washed thrice with PBS. The adherent platelets were then fixed with 3 vol% glutaraldehyde in PBS solution overnight at 4 °C. After serial dehydration with 10%, 25%, 50%, 75%, 90%, and 100% ethanol for 10 min each, the films were dried under reduced pressure, coated with platinum, and observed under SEM. The number of platelets on the films was quantified by counting the total number of adherent platelets from representative SEM images at the same magnification (×2000).[70] The results obtained from the modified films were normalized by that from pristine silicone.

Plasma Recalcification Time (PRT): Fresh blood from a healthy rabbit mixed with 3.8 wt% sodium citrate solution was prepared as described above. The platelet poor plasma (PPP) was obtained by centrifuging the blood at 3000 rpm and 8 °C for 20 min, and the PPP (0.1 mL) was introduced on the surface of a 2 × 2 cm^2 silicone film. After the film was incubated at 37 °C for 10 min, 0.025 M $CaCl_2$ aqueous solution (0.1 mL) at 37 °C was then added to the PPP on the silicone film. The PPP solution was monitored for clotting by manually dipping a stainless-steel wire hook coated with silicone into the solution to detect fibrin threads. The PRT was recorded at the first appearance of silky fibrin.

Hemolysis Test: Silicone film of size 1 × 1 cm^2 and PBS (10 mL) was introduced into a Biologix® centrifuge tube. After the tube was incubated at 37 °C for 1 h, diluted rabbit blood (8 mL of blood mixed with 10 mL of PBS, 0.2 mL) was added and the tube was incubated at 37 °C for another 1 h. PBS and doubly distilled water were used for negative and positive controls, respectively. The tube was then centrifuged at 1500 rpm for 10 min and the optical absorbance of the supernatant was measured at 545 nm on a Hitachi spectrophotometer (Model U-2800). The hemolysis rate (HR) was calculated as follows:

$$HR = (AS - AN)/(AP - AN) \quad (2)$$

where AS, AN, and AP are the optical absorbance of the supernatant of the solution containing film, the negative control and the positive control, respectively.

Characterization: Due to the curved surface of the catheter, characterization methods such as XPS and contact angle measurement as well as SEM observation of adherent bacterial cells could not be easily carried out on its surface. Thus, flat medical grade silicone sheet was selected as a model surface, and after modification, investigation of the coating characteristics was carried out. The surface chemical composition of the silicone films was analyzed by XPS on an Axis $Ultra^{DLD}$ spectrometer (Kratos Analytical Ltd., UK) with a monochromatic Al Kα X-ray source (1486.71 eV photons). The silicone film surfaces were observed by SEM (JEOL, Model 5600 LV), and the cross-sections of films and catheters were observed by FESEM (JEOL, Model JSM-6700) and SEM, respectively. The samples were fixed on the SEM metal stubs using double-sided carbon tapes and sputter-coated with a thin platinum layer to enhance the contrast and quality of the images prior to SEM and FESEM observation. The concentration of the immobilized heparin on the modified films was quantified using the toluidine blue method as described previously.[71] Static contact angles of the different surfaces were measured at room temperature by the sessile drop method using a 3 μL water droplet in a Ramé-Hart telescopic goniometer (Model 100–00-(230)). For each sample, three measurements from different regions of a surface were taken, and at least three independent tests were carried out with triplicate samples each time.

Statistical Analysis: The results were reported as mean ± standard deviation (SD) and were assessed statistically using one-way analysis of variance (ANOVA) with Tukey post hoc test. Statistical significance was accepted at $P < 0.05$.

Supporting Information

Supporting Information is available from the Wiley Online Library or from the author.

Acknowledgements

This work was financially supported by the National Kidney Foundation of Singapore Grant NKFRC/2010/01/07.

Received: July 3, 2013
Revised: August 14, 2013
Published online: November 11, 2013

[1] J. M. Bargman, *Semin. Dial.* **2012**, *25*, 545.
[2] A. Pletinck, R. Vanholder, N. Veys, W. Van Biesen, *Nat. Rev. Nephrol.* **2012**, *8*, 542.
[3] B. Piraino, *Nat. Rev. Nephrol.* **2010**, *6*, 259.
[4] F. H. Bender, J. Bernardini, B. Piraino, *Kidney Int.* **2006**, *70*, S44.
[5] P. K. T. Li, C. C. Szeto, B. Piraino, J. Bernardini, A. E. Figueiredo, A. Gupta, D. W. Johnson, E. J. Kuijper, W. C. Lye, W. Salzer, F. Schaefer, D. G. Struijk, *Periton. Dialysis Int.* **2010**, *30*, 393.
[6] S. J. Nessim, *Semin. Nephrol.* **2011**, *31*, 199.
[7] J. Y. Xie, H. Ren, K. Kiryluk, N. Chen, *Am. J. Kidney Dis.* **2010**, *56*, 1006.
[8] R. Dell'Aquila, S. Chiaramonte, M. P. Rodighiero, E. Spanó, P. Di Loreto, C. O. Kohn, D. Cruz, N. Polanco, D. Kuang, V. Corradi, M. De Cal, C. Ronco, *Periton. Dialysis Int.* **2007**, *27*, S119.
[9] F. Paladini, M. Pollini, D. Deponti, A. Di Giancamillo, G. Peretti, A. Sannino, *J. Mater. Sci.-Mater. Med.* **2013**, *24*, 1105.
[10] F. Paladini, M. Pollini, A. Tala, P. Alifano, A. Sannino, *J. Mater. Sci.-Mater. Med.* **2012**, *23*, 1983.
[11] K. Bazaka, M. V. Jacob, R. J. Crawford, E. P. Ivanova, *Appl. Microbiol. Biotechnol.* **2012**, *95*, 299.
[12] J. Hasan, R. J. Crawford, E. P. Lvanova, *Trends Biotechnol.* **2013**, *31*, 31.
[13] S. Sheikh, D. Y. Yang, C. Blaszykowski, M. Thompson, *Chem. Commun.* **2012**, *48*, 1305.
[14] C. Blaszykowski, S. Sheikh, M. Thompson, *Chem. Soc. Rev.* **2012**, *41*, 5599.
[15] S. El Habnouni, V. Darcos, X. Garric, J. P. Lavigne, B. Nottelet, J. Coudane, *Adv. Funct. Mater.* **2011**, *21*, 3321.
[16] X. Ding, C. Yang, T. P. Lim, L. Y. Hsu, A. C. Engler, J. L. Hedrick, Y. Y. Yang, *Biomaterials* **2012**, *33*, 6593.
[17] J. Duvigneau, S. Cornelissen, N. B. Valls, H. Schonherr, G. J. Vancso, *Adv. Funct. Mater.* **2010**, *20*, 460.
[18] P. M. Imbesi, J. A. Finlay, N. Aldred, M. J. Eller, S. E. Felder, K. A. Pollack, A. T. Lonnecker, J. E. Raymond, M. E. Mackay, E. A. Schweikert, A. S. Clare, J. A. Callow, M. E. Callow, K. L. Wooley, *Polym. Chem.* **2012**, *3*, 3121.
[19] P. M. Imbesi, N. V. Gohad, M. J. Eller, B. Orihuela, D. Rittschof, E. A. Schweikert, A. S. Mount, K. L. Wooley, *ACS Nano* **2012**, *6*, 1503.
[20] R. S. Kane, P. Deschatelets, G. M. Whitesides, *Langmuir* **2003**, *19*, 2388.
[21] I. Banerjee, R. C. Pangule, R. S. Kane, *Adv. Mater.* **2011**, *23*, 690.
[22] Q. S. Liu, A. Singh, R. Lalani, L. Y. Liu, *Biomacromolecules* **2012**, *13*, 1086.
[23] C. Rodriguez-Emmenegger, M. Houska, A. B. Alles, E. Brynda, *Macromol. Biosci.* **2012**, *12*, 1413.
[24] Y. Chang, Y. J. Shih, C. J. Lai, H. H. Kung, S. Y. Jiang, *Adv. Funct. Mater.* **2013**, *23*, 1100.
[25] J. H. Kuang, P. B. Messersmith, *Langmuir* **2012**, *28*, 7258.
[26] R. S. Smith, Z. Zhang, M. Bouchard, J. Li, H. S. Lapp, G. R. Brotske, D. L. Lucchino, D. Weaver, L. A. Roth, A. Coury, J. Biggerstaff, S. Sukavaneshvar, R. Langer, C. Loose, *Sci. Transl. Med.* **2012**, *4*, 153ra132.

[27] A. J. Keefe, N. D. Brault, S. Y. Jiang, *Biomacromolecules* **2012**, *13*, 1683.
[28] S. H. Lin, B. Zhang, M. J. Skoumal, B. Ramunno, X. P. Li, C. Wesdemiotis, L. Y. Liu, L. Jia, *Biomacromolecules* **2011**, *12*, 2573.
[29] A. R. Statz, J. H. Kuang, C. L. Ren, A. E. Barron, I. Szleifer, P. B. Messersmith, *Biointerphases* **2009**, *4*, FA22.
[30] T. H. Dai, M. Tanaka, Y. Y. Huang, M. R. Hamblin, *Expert Rev. Anti-Infect. Ther.* **2011**, *9*, 857.
[31] T. H. Dai, G. P. Tegos, M. Burkatovskaya, A. P. Castano, M. R. Hamblin, *Antimicrob. Agents Chemother.* **2009**, *53*, 393.
[32] P. Li, Y. F. Poon, W. F. Li, H. Y. Zhu, S. H. Yeap, Y. Cao, X. B. Qi, C. C. Zhou, M. Lamrani, R. W. Beuerman, E. T. Kang, Y. G. Mu, C. M. Li, M. W. Chang, S. S. J. Leong, M. B. Chan-Park, *Nat. Mater.* **2011**, *10*, 149.
[33] J. Benesch, P. Tengvall, *Biomaterials* **2002**, *23*, 2561.
[34] R. Lieder, M. Darai, M. B. Thor, C. H. Ng, J. M. Einarsson, S. Gudmundsson, B. Helgason, V. S. Gaware, M. Masson, J. Gislason, G. Orlygsson, O. E. Sigurjonsson, *J. Biomed. Mater. Res. A* **2012**, *100A*, 3392.
[35] P. Tenke, C. R. Riedl, G. L. Jones, G. J. Williams, D. Stickler, E. Nagy, *Int. J. Antimicrob. Agents* **2004**, *23*, S67.
[36] X. E. Chen, P. X. Ling, R. S. Duan, T. M. Zhang, *Carbohydr. Polym.* **2012**, *88*, 1288.
[37] R. M. Q. Shanks, N. P. Donegan, M. L. Graber, S. E. Buckingham, M. E. Zegans, A. L. Cheung, G. A. O'Toole, *Infect. Immun.* **2005**, *73*, 4596.
[38] M. Tasso, S. L. Conlan, A. S. Clare, C. Werner, *Adv. Funct. Mater.* **2012**, *22*, 39–47.
[39] N. Aldred, A. S. Clare, *Biofouling* **2008**, *24*, 351.
[40] Z. Z. Khaing, C. E. Schmidt, *Neurosci. Lett.* **2012**, *519*, 103.
[41] N. J. Meilander-Lin, P. J. Cheung, D. L. Wilson, R. V. Bellamkonda, *Tissue Eng.* **2005**, *11*, 546.
[42] N. Wang, X. S. Wu, *Int. J. Pharm.* **1998**, *166*, 1.
[43] D. J. Stickler, J. C. Lear, N. S. Morris, S. M. Macleod, A. Downer, D. H. Cadd, W. J. Feast, *J. Appl. Microbiol.* **2006**, *100*, 1028.
[44] K. Rasmussen, P. R. Willemsen, K. Ostgaard, *Biofouling* **2002**, *18*, 177.
[45] E. P. Everaert, H. C. VanderMei, H. J. Busscher, *J. Adhes. Sci. Technol.* **1996**, *10*, 351.
[46] Y. J. Kim, I. K. Kang, M. W. Huh, S. C. Yoon, *Biomaterials* **2000**, *21*, 121.
[47] N. J. Hickok, I. M. Shapiro, *Adv. Drug Deliv. Rev.* **2012**, *64*, 1165.
[48] C. Gómez-Suárez, H. J. Busscher, H. C. van der Mei, *Appl. Environ. Microbiol.* **2001**, *67*, 2531.
[49] M. K. Dasgupta, *Semin. Dial.* **2002**, *15*, 338.
[50] A. M. Pereira, A. C. Abreu, M. Simoes, *J. Microbiol. Res.* **2012**, *2*, 84.
[51] L. M. Zhang, C. X. Wu, J. Y. Huang, X. H. Peng, P. Chen, S. Q. Tang, *Carbohydr. Polym.* **2012**, *88*, 1445.
[52] D. Collins, A. M. Hogan, D. O'Shea, D. C. Winter, *J. Gastrointest. Surg.* **2009**, *13*, 1138.
[53] A. Sousa, F. Sousa, J. A. Queiroz, *J. Sep. Sci.* **2012**, *35*, 3046.
[54] H. Mohri, T. Ohkubo, *Arch. Biochem. Biophys.* **1993**, *303*, 27.
[55] T. Hattori, K. Kimura, E. Seyrek, P. L. Dubin, *Anal. Biochem.* **2001**, *295*, 158.
[56] C. Tedjo, K. G. Neoh, E. T. Kang, N. Fang, V. Chan, *J. Biomed. Mater. Res. A* **2007**, *82A*, 479.
[57] C. Wolz, D. McDevitt, T. J. Foster, A. L. Cheung, *Infect. Immun.* **1996**, *64*, 3142.
[58] P. Koegler, A. Clayton, H. Thissen, G. N. C. Santos, P. Kingshott, *Adv. Drug Deliv. Rev.* **2012**, *64*, 1820.
[59] A. W. Bridges, N. Singh, K. L. Burns, J. E. Babensee, L. A. Lyon, A. J. Garcia, *Biomaterials* **2008**, *29*, 4605.
[60] E. De Candia, R. De Cristofaro, R. Landolfi, *Circulation* **1999**, *99*, 3308.
[61] E. Brynda, M. Houska, M. Jirouskova, J. E. Dyr, *J. Biomed. Mater. Res.* **2000**, *51*, 249.
[62] M. Bauer, C. Lautenschlaeger, K. Kempe, L. Tauhardt, U. S. Schubert, D. Fischer, *Macromol. Biosci.* **2012**, *12*, 986.
[63] A. Pourjavadi, S. S. Afjeh, F. Seidi, H. Salimi, *J. Appl. Polym. Sci.* **2011**, *122*, 2424.
[64] D. S. W. Benoit, A. R. Durney, K. S. Anseth, *Biomaterials* **2007**, *28*, 66.
[65] Z. L. Shi, K. G. Neoh, E. T. Kang, W. Wang, *Biomaterials* **2006**, *27*, 2440.
[66] Z. L. Shi, K. G. Neoh, E. T. Kang, C. Poh, W. Wang, *J. Biomed. Mater. Res. Part A* **2008**, *86A*, 865.
[67] T. Monsen, E. Lovgren, M. Widerstrom, L. Wallinder, *J. Clin. Microbiol.* **2009**, *47*, 2496.
[68] J. Hankiewi, E. Swiercze, *Clin. Chim. Acta* **1974**, *57*, 205.
[69] I. K. Kang, B. K. Kwon, J. H. Lee, H. B. Lee, *Biomaterials* **1993**, *14*, 787.
[70] C. C. Tsai, Y. Chang, H. W. Sung, J. C. Hsu, C. N. Chen, *Biomaterials* **2001**, *22*, 523.
[71] R. A. Hoshi, R. Van Lith, M. C. Jen, J. B. Allen, K. A. Lapidos, G. Ameer, *Biomaterials* **2013**, *34*, 30.